

## Structure and Properties of the S49 Rail After a Long Term Outdoor Exposure

Jarosław Konieczny<sup>1\*</sup>, Krzysztof Labisz<sup>1</sup>

<sup>1</sup> Department of Railway Transport, Faculty of Transport and Aviation Engineering, Silesian University of Technology, ul. Krasińskiego 8, 40-019 Katowice, Poland

\* Corresponding author's e-mail: [jaroslaw.konieczny@polsl.pl](mailto:jaroslaw.konieczny@polsl.pl)

### ABSTRACT

The subject of the research in this work was the S49 rail made of R260 rail steel (1.0623). The carried out investigations concern microstructure tests and tests of mechanical properties of rails after several years of exposure in the open air without usage. The purpose of the work was to determine on the basis of the results of research the possibilities of using the tested rail for usage and application for the construction of tracks on railway sidings. For investigations there were used diverse techniques reaching such engineering materials investigations like light or scanning electron microscope for microstructure investigations, as well as hardness and microhardness test were performed for determinations of the microstructural changes occurred in the upper area of the rails surface. The microstructure changes concerns especially the ferritic and pearlitic structure and the breaks in the present carbide mesh. During investigations it was found out that the tested railway rails are fully useful for application, after machining to achieve required dimensional parameters. It is also of high importance, of the economical point of view, that their price, also in case of earlier installation of the rails, may be lower than the current price offered on the market for a entire new product. The price difference reaches dimensions in the range of 5–10%.

**Keywords:** microstructure, perlite, ferrite, hardness.

### INTRODUCTION

The selection of materials for rails and railway surface should depend on the load and pressure applying on the rail, travel speed and frequency of transport, which will ensure lower wear and longer durability of turnouts and railway tracks [1, 2].

One of the ways to increase the abrasion resistance of pearlitic steels is to modify its morphology, e.g. by means of isothermal annealing parameters [3]. Increasing the wear resistance can also be realized by improving the cleanliness of steel and increasing the carbon content [4] as well as head hardening the rails [4–6].

Another issue is the fact, that different sections of the route have different susceptibility to the key mechanisms of rail degradation, which was demonstrated in the work [7]. The degradation results in a deterioration in the quality of the

track geometry and this results in high dynamic vibrations of the vehicle and the track and the loss of geometrical compatibility between track and wheel leading to a higher probability of derailment. For these reasons, the quality of track geometry affects driving safety, wear of cooperating elements, and vibrations that cause noise. Track parameters are defined in European standards to harmonize the European rail network [8, 9].

The question that railroad managers ask themselves, in this case concerning siding, is: Is it possible to use previously used rails instead of new ones, e.g. on a railway siding where the maximum permitted train speed is 40 km/h [10, 11]. Although the speeds values reaching above 30 km/h on the sides are considered as high [8]. Especially if it is possible to buy rails that were once midwives on the trail, but due to the fact that traffic on the trail has been suspended, they

have virtually no signs of wear. The use of such rails is justified primarily for economic reasons [12]. If the provisions and recommendations contained in references [13] are taken into account, it turns out that if 200,000 tonnes of coal are transported annually on the siding, the  $Tg = 0.2$  freight rate and new rails should be used for the construction of tracks with  $Tg = 16\div 25$  freight rate per year. In the area of expenditure, the construction of 1 km of track using new rails will cost about 450,000. PLN [12].

Railway sidings are a key element of the infrastructure of large plants, such as coal mines, production plants or intermodal facilities, such as ports, road-rail or sea-rail terminals [8].

Railway sidings, unlike other railway routes, are characterized by a limited length and speed of operation, and only freight wagons are transported. On the infrastructure side, there is a high density of turnouts and frequent changes in track curvature.

Of course, the outdoor exposure of the rails for several years meant that they were covered with a layer of rust. Therefore, before making a decision on purchasing such rails, it should be checked whether they meet the technical conditions for the construction and collection of rail rails, in accordance with the requirements of the PKP PLK Railway Road Office [13].

The power function, also known as the bilogarithmic law, is used to predict atmospheric corrosion of metal materials, even after long exposure times. The accuracy and credibility of this relationship has been confirmed by many authors [14–17]. Atmospheric corrosion in an industrial environment can be described by the equation [15, 18, 19]:

$$C = At^n \quad (1)$$

or its logarithmic transformation:

$$\ln C = \ln A + n \ln t \quad (2)$$

where:  $C$  - corrosion after time  $t$ ;  $A$ ,  $n$  – constants.

The value of  $n$  can be a criterion for assessing long-term susceptibility to atmospheric corrosion. It gives a measure of the resistance to transport processes within the product oxide corrosion after its formation. When  $n$  is close to 0.5, this may be due to an ideal diffusion controlled mechanism with all corrosion products remaining on the metal surface. This seems to be the case on slightly polluted atmospheric land [19].

In the example discussed in the article, the constant  $A$  of  $60 \mu\text{m}$  [43] was adopted for the rail made of R260 steel.

Substituting the values of  $n=0.5$  and  $A=60 \mu\text{m}$  and  $C=160 \mu\text{m}$  [36] as the limit value in the industrial environment according to the PKP guidelines, the result was  $t = 7.07$  years. This result expresses the maximum aging time of the rail enabling its re-use after re-profiling.

The application of grinding in practice is often used as one of the maintenance processes to re-profile the rails and remove damage to the surface of the rails, e.g. in the event of a fatigue crack or rail head inspection, in some cases the technique can significantly change the mechanical properties of the surface and material of the rail base affecting the overall reusability of the splint. The abrasive used and the stress can be decisive factors in the properties and surface of the rail material after grinding. The problem resulting from the use of improperly selected grinding conditions is also the occurrence of decarbonisation. The decarbonized layer is essentially a layer produced by environmental effects on the surface of the rail. The result is that this layer appears white under the rail surface [20, 21].

In the presence of air, iron oxidizes to  $\text{Fe}_3\text{O}_4$ , which results in a layer of scale on the surface. The carbon in steel also reacts with oxygen. Below the A1-3 temperature (Fe- $\text{Fe}_3\text{C}$  system) this process takes place slowly, and above the temperature it accelerates, the faster the higher the temperature. Each of the components present in the air:  $\text{O}_2$ ,  $\text{CO}_2$ ,  $\text{H}_2\text{O}$  is both oxidizing and decarburizing. This is confirmed by the conclusions in [22] where it was found that when carbon steel was hot rolled to the desired rail profile at  $1200 \text{ }^\circ\text{C}$ , it can decarburize on the surface of the rail because the oxidation of carbon is faster than that of iron. Moreover, in [23] found that decarburization is present on all new rails and, unless polished down, will be on the rail running surface after installation and continue.

In addition, it should be noted that the Procedure of Covering the Railway Siding Safety Certificate (in Polish “Procedura Objęcia Certyfikatem Bezpieczeństwa Bocznic Kolejowej”) involves the description of siding infrastructure and the specification of the requirements that they should meet, taking into account, among others construction standards of track surface and technical characteristics of rails; it is also necessary to develop requirements for maintaining the proper technical condition of the siding (including permissible values of rail wear) [24].

## MATERIALS AND METHOD

The analysis presented in the article was developed based on the results of microstructure investigations, performed on a light microscope, using the Leica light field testing technique with a dedicated image processing software in the 50–200× magnification range. Also measuring of the hardness of the S49 rail (Fig. 1) made of R260 rail steel was performed. The rail was put on the tracks immediately after being purchased from the manufacturer and lay on tracks that had not been operated for 5 years.

The chemical composition of steel of the tested rail according to the railway standard [25] is presented in Table 1.

The R260 rail steel is characterized by a hardness of 260–300 HBS [26]. The hardness measurement was carried out on a Zwick hardness tester in accordance with the recommendations [4] (Fig. 2) contained in the EN ISO 10003-1 standard [27]. The surface of the samples before measurement was properly prepared by polishing on 200–1200 wet abrasive paper on a mechanical grinding-polishing machine.

The material for the tests was taken from the rail cross-section in accordance with the requirements of the Technical Conditions for the Performance and Collection of Rail Rails [13] (Fig. 3). The collected material was hot embedded in a thermoplastic polymer and after grinding and



Fig. 1. Fragment of the investigated S49 rail

Table 1. Chemical composition of R260 rail steel [25]

| Chemical elements | Concentration of alloying elements, % |          |           |                  |      |                   |      |
|-------------------|---------------------------------------|----------|-----------|------------------|------|-------------------|------|
|                   | C                                     | Si       | Mn        | P <sub>max</sub> | S    | Al <sub>max</sub> | Mo   |
| concentration     | 0.6÷0.8                               | 0.13÷0.6 | 0.65÷1.25 | 0.03             | 0.03 | 0.004             | 0.02 |

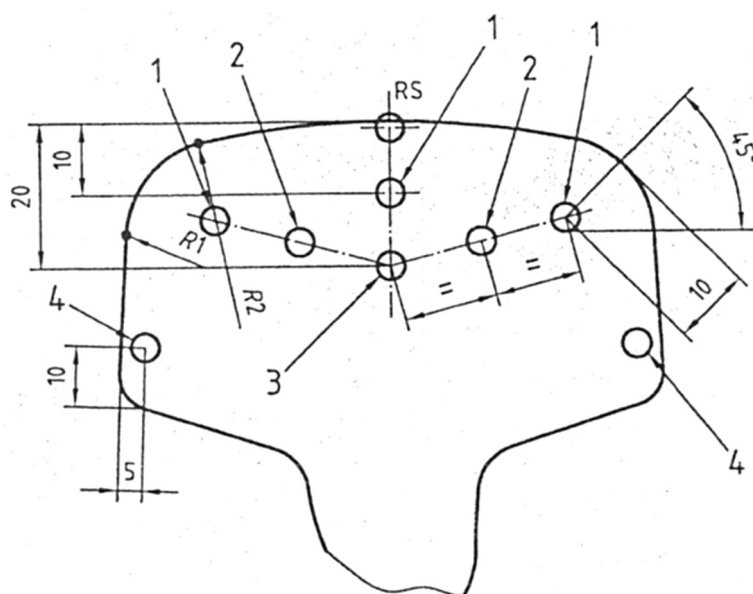


Fig. 2. Arrangement of hardness test points according to [13]

polishing using a dedicated program on a mechanical grinding-polishing machine using an abrasive agent with a gradation of 1–6  $\mu\text{m}$  and lubricant. After the polishing process, the samples were etched with a 5% Nital solution at room temperature for 40s.

### INVESTIGATION RESULTS

In accordance with the requirements contained in the Technical Conditions for the Making and Receiving of Rail Rails [13], the hardness on the centre line of the running surface of the rail head (at the RS point) should be in the range of 260–300 HBS. The measurement results showed that

the hardness of the tested rail meets the necessary conditions for using the rail for track construction (Fig. 4, Table 2). It is also worth to mention that the standard deviation of the measurements obtained in the required places is in the range of 2.0–6.7, which is 0.6–2.2% of the average value. This proves that the difference between successive measurement results is below the statistical error, it results from the fact that the tested rail over the entire cross-section is characterized by uniform values of the measured hardness.

Measured microhardness is presented in Figure 5, where the values decrease is visible, beginning from the relatively low level of up to 200  $\text{HV}_{0.05}$  in the decarbonizes layer going through a transition zone to the basic value of the rail core

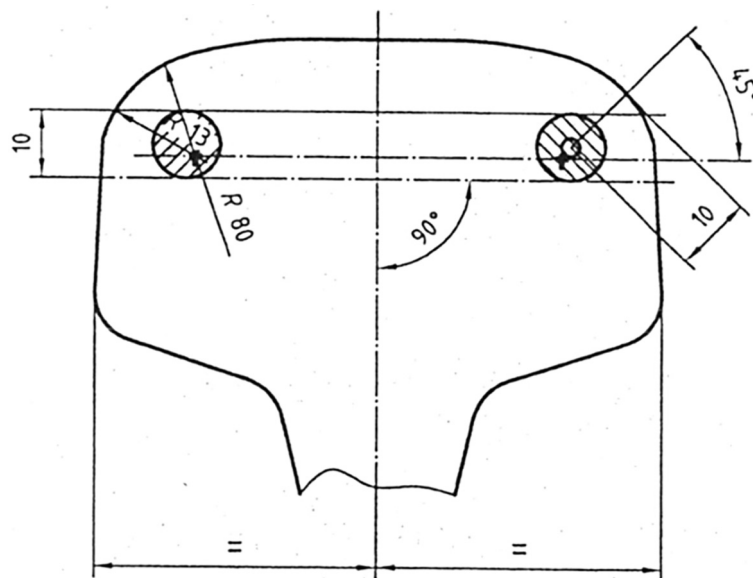


Fig. 3. Place of sampling for microstructure checking and samples for tensile strength testing [13]

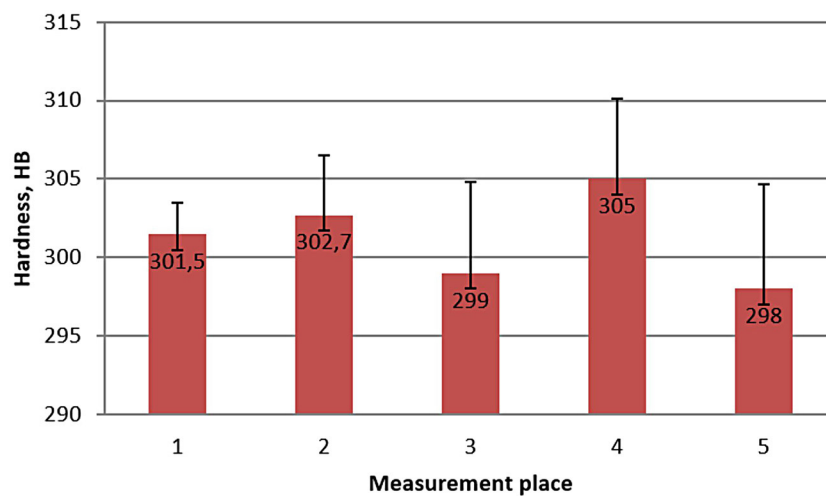


Fig. 4. Results of hardness measurement and standard deviation of the tested rail steel; measurement point 5 is related to RS area on Fig. 2

**Table 2.** Hardness test results

| Place of measurement | Hardness HBS | Standard deviation |
|----------------------|--------------|--------------------|
| RS                   | 301.5        | 2.0                |
| 1                    | 302.7        | 3.8                |
| 2                    | 299          | 5.8                |
| 3                    | 305          | 5.1                |
| 4                    | 298          | 6.7                |

reaching a value ca up to 300 HV<sub>0.05</sub>. There is visible a clear decies of the microhardness, related to the decarbonisation level in to a depth of 500 µm corresponding also with the obtained microstructures. On the top of the surface layer the microhardness is relatively stable in range of ca 180–200 HV<sub>0.05</sub> in to a depth of 300 µm. On this basis the decarbonisation can be confirmed and is similar to the microstructure related to the depth form surface presented on micrographs in Figures 7a and 7b.

Metallographic microscopic tests of the supplied rails manufactured from the R260 steel grade were carried out in accordance with the standard [28] and the samples were taken according to the recommendations contained in the Technical Conditions for the Production and Collection of Rail Rails [13]. As a result of the tests performed, a pearlitic structure with ferrite precipitations (white) in the form of a closed ferrite mesh (Fig. 6a) was visualized in the cross-sectional structure at the rail surface. It was found that the ferrite mesh occurs in the band at a depth of up to about 0.5 mm from the running surface of the rail head and with the distance from the

running surface of the head, the ferrite separation mesh no longer closes all grains (Fig. 6b) and finally disappears completely (Fig. 7).

No ferrite precipitates were found in the remaining area of the microstructure (Fig. 7a). The structure of the tested rail did not have the structure of martensite, bainite or cementite (Fig. 7b), which is in accordance with the requirements set out in the Technical Conditions for the Production and Collection of Rail Rails [13].

Figure 6 shows the places from which samples were taken for tests on the microscope. Decarburization occurred in form of closed ferrite mesh is visible in the area of 400–500 µm from the rail head surface.

The presence of a decarbonised layer (Fig. 7, 9a) is well known, but its formation is still under investigation. Three occurrence of decarbonisation have been explained as reaction of the material surface with the environment also by oxidation. Much research has been done to elucidate the mechanisms and their effect on material performance and service life. Currently, it is argued that a mechanism can be used to explain this phenomenon, which is based on the combined action of friction and heat and dislocation that occurs as a result of plastic deformation. An additional factor affecting the quality of the material after long-term use is also the size and directionality of the pearlitic areas, in particular the direction of the ferrite plates (Fig. 9b, Table 3) which in the tested material indicates a relatively homogeneous character. On Figure 10 are presented microstructure obtained using the scanning electron microscope. There are visible large ferrite and perlite areas,

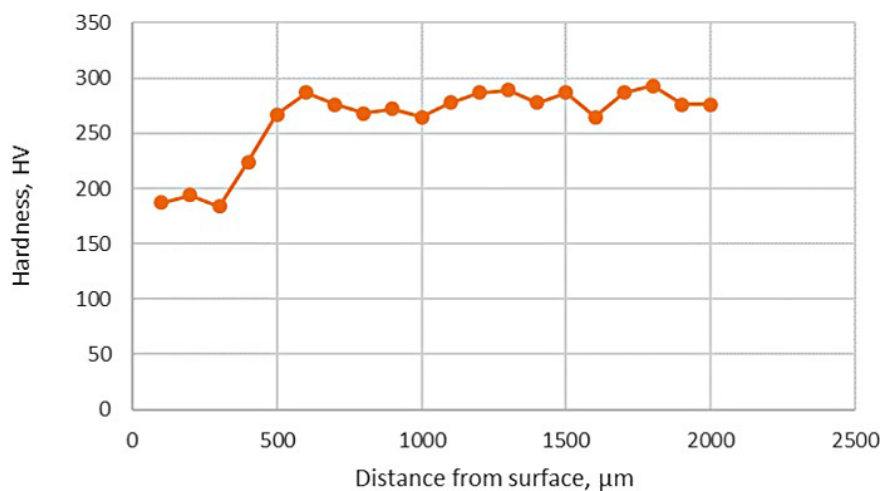


**Fig. 5.** Results of micro-hardness measurement and standard deviation of the tested rail steel measured in point RS, as shown in Fig. 3

confirming the occurrence of these phases in the microstructure of the investigated material.

Concerning the question of the influence of mechanical properties of the pearlitic rail steel with fine interlamellar spacing it is worth to underline, that they can be determined and calculated from the following equations (3) [29]:

$$\delta_y = 295.5 + 114.2\chi^{-1} \quad (3)$$

where:  $\chi = (2S_0-t)$ ;  $t$  – thickness of the cementite plate calculated as  $0.015S_0$  [C].

Using this relationship it can be summarised, that the smaller the perlite plates size, the higher the mechanical properties – strength of the rails head surface. It is also possible to determine the size of those structural components using the following equation (4).

$$S_0 = \frac{1}{a - bT_p} \quad (4)$$

where:  $a, b$  – coefficients;  $T_p$  – volume fractions of pearlite.

On the basis of research results, H. Yokoyama et al. [30] stated that, contrary to the generally accepted view, fine-tuning the size of the perlite areas effectively improves wear and damage resistance. Wear resistance increased along with the fragmentation of the perlite areas. Lamellar

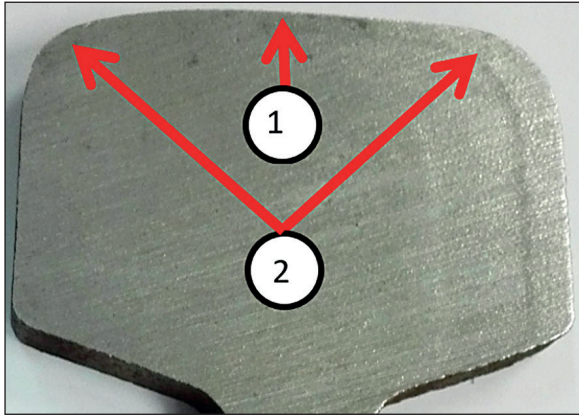


Fig. 6. Cross-section of the head of the tested S49 rail, where the material for sampling is taken

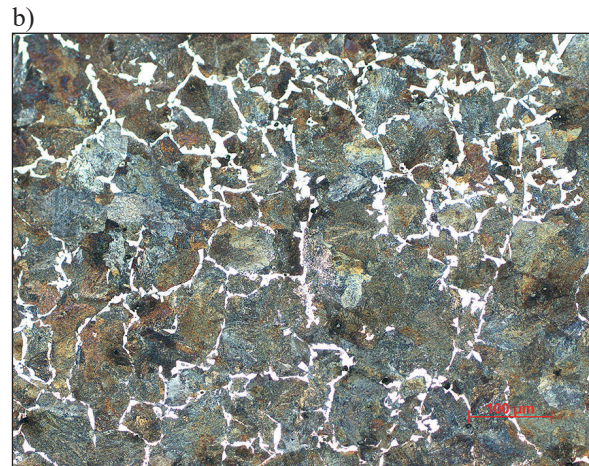
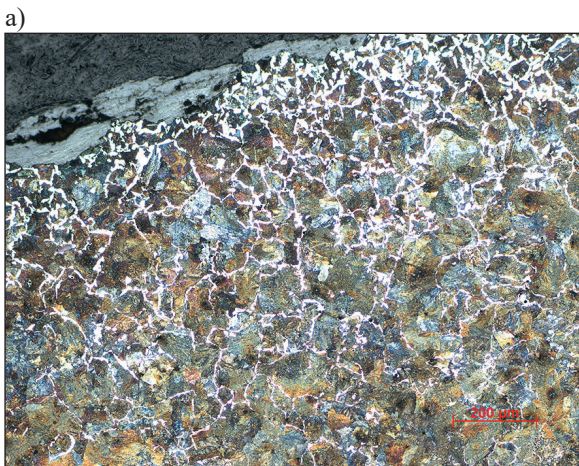


Fig. 7. Microstructure on the cross-section of the rail at the surface of the rail head from area 1 in Fig. 6

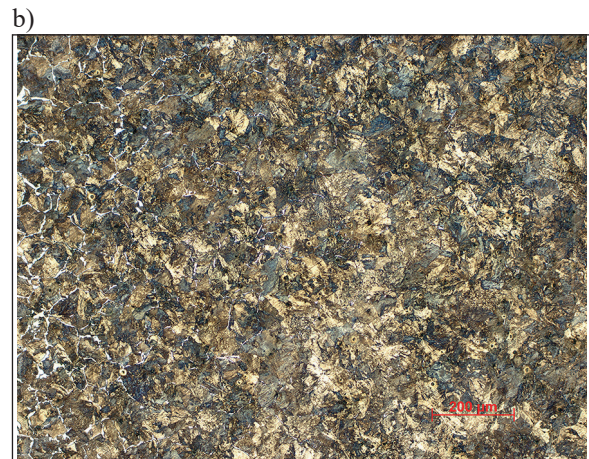
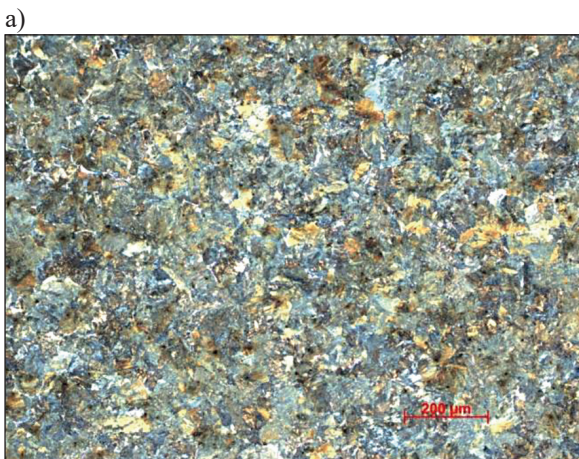


Fig. 8. The microstructure of the tested S49 rail from area 2 in Fig. 6

structures, when subjected to plastic deformation, are characterized by significant anisotropy determined by the lamellar direction. For this reason, there is a high concentration of stresses along the boundaries of the areas, which are the sites of crack formation. Similar results were obtained in [31], in which the authors confirmed that the wear resistance of R260 steel with a pearlitic structure depends on the perlite morphology - the distance between the plates in the cementite and the thickness of the lamellas (Table 3). In this work perlite areas (grains) were also confirmed in the decarbonised surface layer (Fig. 7a and 7b).

These parameters can be adjusted by heat treatment - isothermal annealing or plastic working – hot rolling [32]. Moreover, it was also found that the abrasion resistance of R260 steels with a

pearlitic structure and different perlite morphology decreased with increasing load and slip.

The use of solid lubricants for the lubrication of the flanges of railway wheels may also contribute to the formation of corrosive defects on the rail head surface [33].

In the work [34] it was found that in the samples taken from the exploited section of rail made of R260 steel with large deformations present close to the surface, there is a large hardness gradient with high hardness close to the surface, which is most likely the result of work hardening.

In the presented article occurrence of cracks has not been confirmed, however the other authors have detected and analysis this phenomenon. The influence of grain boundaries between perlite and ferrite on crack propagation caused

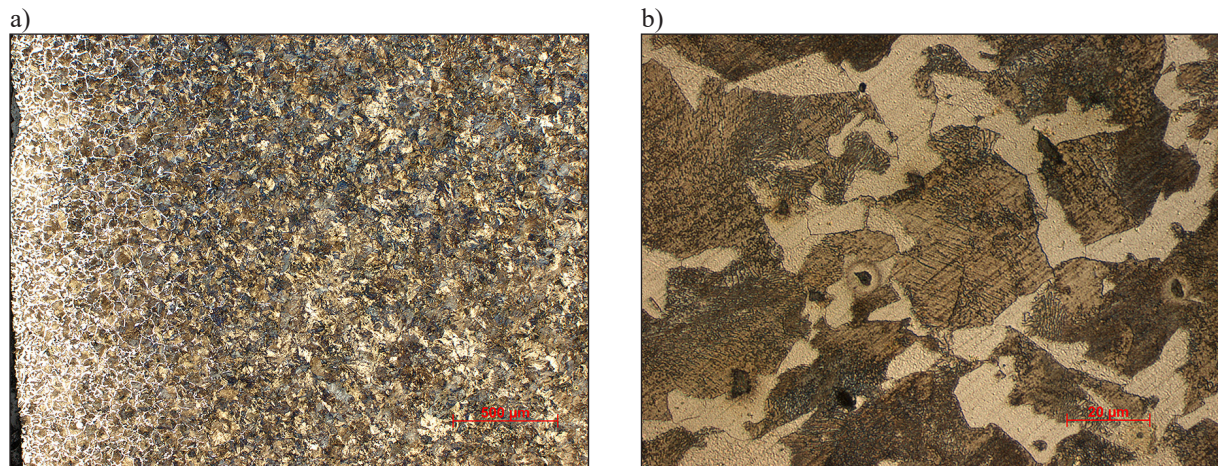


Fig. 9. a) Decarbonised layer on the left fig site, b) perlite plates direction

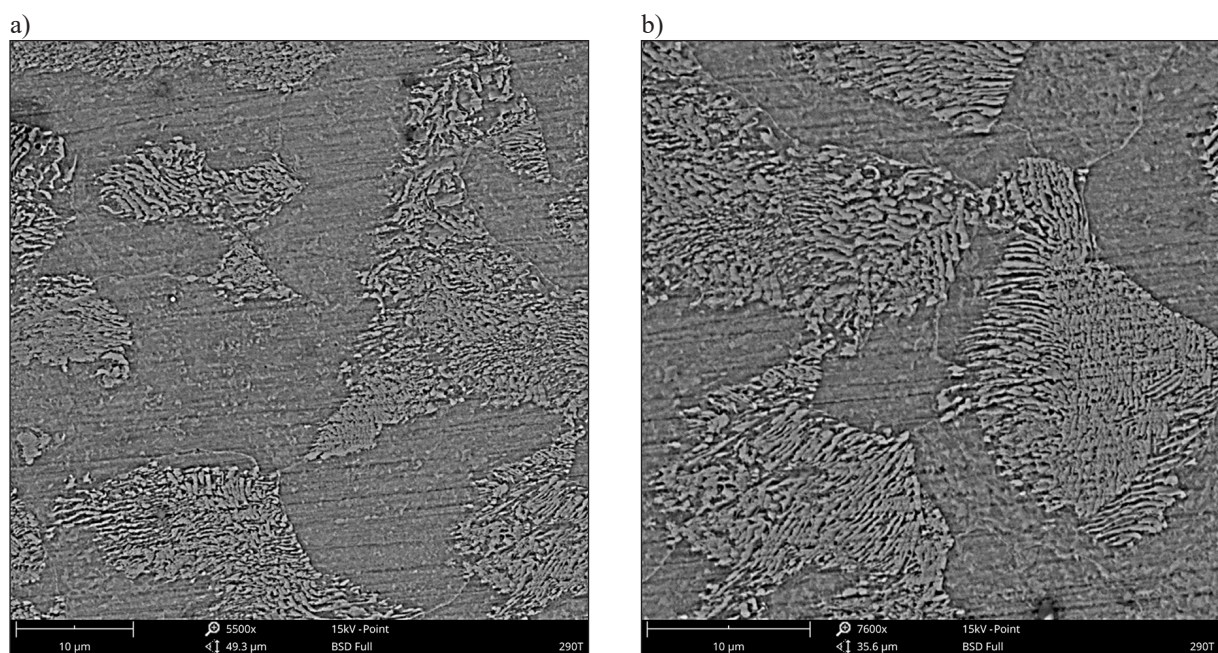


Fig. 10. Microstructure of the investigated rail steel, SEM

by rolling fatigue is presented in [35]. The deformation separation between the proeutectoid ferrite and perlite facilitates the initiation and propagation of cracks during Rolling Contact Fatigue (RCF). Proeutectoid is defined as the first diffusional product to form from austenite upon cooling. This was noticed in the highly hardened state and in the exhaustion of the toughness of the proeutectoid ferrite phase, surface microcracks initiated at the boundary between the stressed ferrite phase and the stressed perlite. The test results presented by Granham and all [35] showed that the higher the content of proeutectoid ferrite in the microstructure of the rail steel, the lower the average durability of RCF crack initiation. The reason for this is that the proeutectoid ferrite deforms faster when the ferrite grains are limited by adjacent perlite nodules.

The required rail cross-section is presented on Figure 11, where the H parameter (maximum deviation from the theoretical contour of the running surface) is set as high as 0.16 mm for old-used rails. In the investigated case this distance is up to 450 μm, what requires mechanical removing of the surface area up to 300 μm, to be used main line, however for sidings line the additional machining is to be smaller or even can be skipping at all.

The determined decarbonization can also affect the defect of head checking (HC), which is the dominant defect from the group of contact-pressure defects (RCF). This defect is caused by fatigue of the material on the running surface of the rail, in the places where the rail co-operates, where the rail is subject to the cyclical load of the passing rolling stock. A predominant shape of rail corrugation is wear at the wave length of 25÷80 mm – so-called „short” waves. For the development of rail corrugation a considerable influence has got an arising resonance of non-sprunged mass (e.g. non-sprunged mass of most loaded freight car) and railway track structure stiffness. Rail corrugation may also be bases on plastic deformation due to the occurrence of decarbonized areas near to the rail head surface. Most often method of rail corrugation elimination is rail reforming in track, i.e. their grinding

by special machines or machines set operated by computer, which create a complex trains for rail grinding. It appears, that grinding of new rails is excellent countermeasure against rail corrugation arising. Additionally the rail reforming removes not only rail corrugation though also the other shapes (e.g. rail contact fatigue) [37, 38].

The luxation may also be a consequence of the decarbonisation of the top layer of the rail head. As this defect most often occurs, for example, before the entry signal, where heavy freight trains are suddenly braked or started, as well as before rail-road crossings and before turnouts [39], decarbonisation causing a decrease in the hardness of the top layer of the rail will make the rail more susceptible for such damage.

In the case of a squat defect manifested by a crack and a local depression of the running surface [40], decarbonisation causing a decrease in hardness, and thus indirectly plasticization of the top layer of the rail head, should not cause cracks in the rails.

As presented in [41], the number of operational damages to the rail running surface increases with the increase in the number of transports and the load on the railway lines. As the tested rails were to be used in the construction of sidings, the probability of the appearance of operational defects is relatively low.

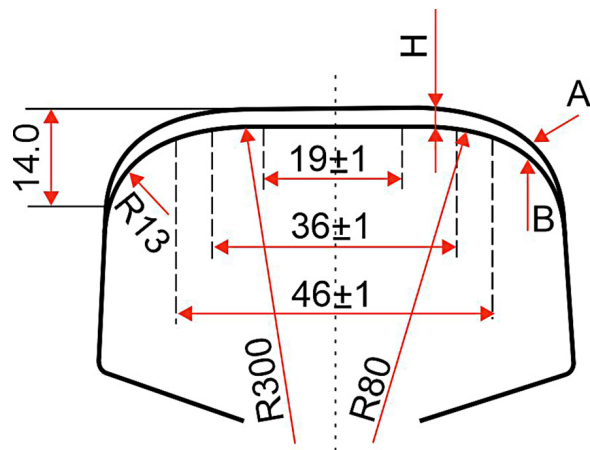


Fig. 11. Scheme of proper rail cross-section with parameters: H – maximum deviation from the theoretical contour of the running surface 49E1 (S49); distance A – B = H = 0.16 mm [36]

Table 3. The distance of the perlite plates in the grains

| Parameters         | 1    | 2    | 3    | 4   | 5    |
|--------------------|------|------|------|-----|------|
| Mean value [μm]    | 9.6  | 10.0 | 12.3 | 5.7 | 10.9 |
| Standard deviation | 0.64 | 1.31 | 2.27 | 0.7 | 2.38 |

The stress level is influenced not only by external factors, but also by the state of own stresses, topography of the rail running surface, all geometric and structural notches (including discontinuities) causing stress concentration. The greatest stresses arise at the top of the rail head.

The appearance and development of damage on the surface of the rail and of the elements working in the rolling-sliding contact depends, on the one hand, on the load and stress level in the most stressed area of the rail (the so-called Bielajev point), and on the other hand, on the material properties, what the rail was made of, and above all, its strength in this area. Exceeding the yield point of the material leads to the formation of subsurface cracks as a result of the plasticization of the material. Thus, the increase in the depth of the decarburization zone reaching the Bielajev point may contribute to the formation of an interfacial boundary at the point of the highest material stress.

## CONCLUSIONS

Based on the tests performed, the rails supplied for testing meet the conditions of use for the construction of tracks on railway sidings. The main finding was related to the determination of the possible duration of the usage time of the long-term aged rail – in the investigated case 5 years – which was determined numerically as high as 7 year, after reprofiling according to the requirements set by the PKP roles. This machining treatment can remove the outer surface layer consisting of the closed ferrite mesh, which was confirmed by metallographic investigation using scanning electron microscopy SEM

As a result of microstructure tests, a uniform uninterrupted ferrite mesh was found in the examined rail material at a depth of up to 0.5 mm from the running surface of the rail head, which indicates that the heat treatment has been properly carried out and there is no visible impact of rail aging in natural conditions.

The hardness tests performed indicate no impact of long-term rail aging on hardness, ranging from 298 to 305 HBS. Also noteworthy is the relatively low value of the measured standard deviation, confirming the homogeneity of the tested microstructure with regard to mechanical properties.

Based on the analyses carried out, it can be stated that the tested railway rails, regardless of

production time/age, are fully useful for mounting on a siding, while maintaining dimensional parameters. It can also be mentioned that their price, irrespective of the fact of their earlier installation, may be lower than the market price of a new product may be lower by approx. 5–10% [12]. In addition, the difference in price is: new rail S49: ca. PLN 3,000, old-use rail: ca. PLN 1,850. (2014) [42].

Concerning the size and perlite arms direction it can be proposed a decrease of the perlite areas size as well as to disorder the growth direction of perlite plates growth during plastic deformation of the rail in production process.

There are not found any cracks or defects of the surface layer, because of the nature of the storage of the rails, so the rail surface need only be to polish in terms of future usage grinding first of the decarbonized layer from the top of the rail.

## REFERENCES

1. Labisz K., Konieczny J. Natural ageing effects on microstructure and properties of rail fastening elements SKL-12. *Scientific Journal of Silesian University of Technology. Series Transport*. 2020; 106: 85–96.
2. Stencel G. Dobór składników nawierzchni kolejowej ze względu na jej trwałość. *Inżynier Budownictwa*. 2013. <https://inzynierbudownictwa.pl/dobor-skladnikow-nawierzchni-kolejowej-ze-wzgledu-na-jej-trwalosc/> (attendance 2021.07.05)
3. Aniołek K., Herian J. The structure, properties and a resistance to abrasive wear of railway sections of steel with a different pearlite morphology. *Technologies and Properties of Modern Utilised Materials. IOP Conf. Series: Materials Science and Engineering*. 2011; 22: 012012
4. Masoumi M., Anderson E., Echeverri A., Tschiptschin A. P., Goldenstein H. Improvement of wear resistance in a pearlitic rail steel via quenching and partitioning processing. *Scientific RepoRts*. 2019; 9: 7454. <https://doi.org/10.1038/s41598-019-43623-7>
5. Zygmunt T., Pietrzyk M., Rauch Ł., Bachniak D. Optimization of the heat treatment process to obtain the required distribution of mechanical properties in the rail head of pearlitic rails. *Journal of Metallic Materials*. 2019; 71(1): 3–9.
6. Josefson B.L., Bisschop R., Messaadi M., Hantusch J. Residual stresses in thermite welded rails: significance of additional forging, *Welding in the world*; 2020.
7. Bevan A., Jaiswal J., Smith A., Ojeda Cabral M. *Judicious Selection of Available Rail Steels to Re-*

- duce Life Cycle Costs. Proceedings of the Institution of Mechanical Engineers. Part F: Journal of Rail and Rapid Transit. 2020; 234(3): 257–275.
8. Licciardello R., Malavasi G., Tieri A., Vitali P. Reference values for railway sidings track geometry. In: 6th Transport Research Arena; 2016; Transportation Research Procedia. 2016; 14: 1996–2005.
  9. Technical Specification for Interoperability of the “Infrastructure” Subsystem of the Railway System in the European Union TSI INF (2014). EN 13848 series.
  10. Instruction on running train traffic Ir-1 (R-1). Annex to Resolution No. 693/2017 of the Management Board of PKP Polskie Linie Kolejowe S.A. of 27 June 2017. (in Polish)
  11. Instructions on shunting technique Ir-9 (R34). PKP Polskie Linie Kolejowe S.A. (in Polish)
  12. Bardziński W. Do you buy new rails or old ones? Part 1.; TOMAX - Comprehensive Railway Siding Services. <http://tormax.com.pl/czy-kupowac-nowe-szyny-czy-staro-uzyteczne-czesc-1/> (in Polish; / attendance 2021.12.03)
  13. Technical Conditions for the Performance and Receipt of Rail Rails, PKP PLK Railway Road Office WTWiO-ILK3-5181-2/2004E.P. (in Polish)
  14. Bohnenkamp K., Burgmann G., Schwenk W. Investigations of the atmospheric corrosion of plain carbon and low alloy steels in industrial, rural and sea air. *Stahl und Eisen*. 1973; 93(22): 1054–1060.
  15. Legault R.A., Preban A.G. Kinetics of the atmospheric corrosion of low-alloy steels in an industrial environment. *Corrosion*. 1975; 31(4): 117–122.
  16. Pourbaix M. The linear bilogarithmic law for atmospheric corrosion, in *Atmospheric Corrosion*. W. H. Ailor, Ed., J. Wiley & Sons; 1982.
  17. Feliu S., Morcillo M. Atmospheric corrosion testing in Spain. In: *Atmospheric Corrosion*. 1982: 913–922.
  18. Legault R.A., Pearson V.P. Atmospheric Corrosion in Marine Environments. *National Association of Corrosion Engineers*. 1978; 34(12): 433–437.
  19. Diaz I., Cano H., Chico B., de la Fuente D., Morcillo M. Some Clarifications Regarding Literature on Atmospheric Corrosion of Weathering Steels. *International Journal of Corrosion*. 2012; 812192.
  20. Mesaritis M., Shamsa M., Cuervo P., Santa J.F., Toro A., Marshall M.B., Lewis R. A laboratory demonstration of rail grinding and analysis of running roughness and wear. *Wear*. 2020; 456–457.
  21. Zhang R., Zheng Ch., Chen Ch., Lv B., Gao G., Yang Z., Yang Y., Zhang F. Study on fatigue wear competition mechanism and microstructure evolution on the surface of a bainitic steel rail. *Wear*. 2021; 482–483: 203978.
  22. Zhao X.J., Guo J., Wang H.Y., Wen Z.F., Liu Q.Y., Zhao G.T., Wang W.J. Effects of decarburization on the wear resistance and damage mechanisms of rail steels subject to contact fatigue. *Wear*. 2016; 364–365: 130–143.
  23. Carroll R.I., Beynon J.H. Decarburization and rolling contact fatigue of a rail steel. *Wear*. 2006; 260: 523–537.
  24. Office of Rail Transport, Certificate of safety of railway sidings. <http://utk.gov.pl/pl/aktualnosci/6151,Objecie-certyfikatem-bezpieczenstwa-bocznic-kolejowych.html> (in Polish)
  25. Polish Standard PN-EN 14811+A1:2009 Railway - Track - Special rails - Grooved rails and related structural profiles.
  26. Tomić-Torlaković M. Guidelines for the rail grade selection. *Metalurgija*. 2014; 53(4): 17–720.
  27. European Standard for the Brinell hardness test for metallic materials. EN ISO 10003-1 – Metal materials - Brinell hardness measurement.
  28. Polish Standard for the sample preparation for macroscopic and microscopic examination and test procedures and their main goals PN-EN ISO 17639:2013-12 – Destructive testing of welded metal joints – Macroscopic and microscopic examination of welded joints. (in Polish)
  29. Kuziak R., Pidvysots’kyy V., Pernach M., Rauch L. Selection of the best phase transformation model for optimization of manufacturing processes of pearlitic steel rails. *Archives of Civil and Mechanical Engineering*. 2019; 19: 535–546.
  30. Yokoyama H., Mitao S., Takemasa M. Development of High Strength Pearlitic Steel Rail (SP rail) with Excellent Wear and Damage Resistance. *Materials Science*. 2002; 176: 59–64.
  31. Herian J., Aniołek K. Abrasive wear of railway sections of steel with a different pearlite morphology in railroad switches. *Journal of Achievements in Materials and Manufacturing Engineering*. 2010; 43(1): 236–243.
  32. Herian J., Aniołek K. The structure and properties of steel with different pearlite morphology and its resistance to abrasive wear. *Archives of Materials Science and Engineering*. 2008; 31(2): 83–86.
  33. Bąkowski H. The influence of solid lubricants used for the lubrication of wheel flanges on railways to reduce the corrosion of rails. *Tribologia*. 2016; 4: 21–28.
  34. Nikas D., Meyer K. A., Ahlström J. Characterization of deformed pearlitic rail steel. In: 8th Risø International Symposium on Materials Science. *Materials Science and Engineering*. 2017; 219: 012035.
  35. Garnham J.E., Franklin F.J., Fletcher D.I., Kapoor A., Davis C.L. Predicting the life of steel rails. In: Proceedings of the Institution of Mechanical Engineers. Part F: Journal of Rail and Rapid Transit. 2007; 221: 45–58.

36. Annex to the order No. 21/2010 of the Management Board of PKP Polskie Linie Kolejowe S.A. dated August 31, 2010; Technical conditions for the manufacture and acceptance of old useful railway rails obtained by regeneration, reprofiling and welding in stationary plants – Requirements and tests Id-107. (in Polish)
37. Bednarek W.A. Wavy railroad wear (causes and remedies). Archives of the Institute of Civil Engineering. 2015; 20: 7–23. (in Polish)
38. Licow R. Assessment of damage to the running surface of railway rails using vibroacoustic phenomena, doctoral dissertation. Poznań University of Technology. Poznań 2018. (in Polish)
39. Licow R., Tomaszewski F. Identification of rail running surface defects with vibroacoustic signal. Railway Problems. 2019; 184: 71–76. (in Polish)
40. Zariczny J., Grulkowski S. Characteristics of defects in rails detected on the railway line No. 131 Chorzów Batory-Tczew with particular emphasis on the defects of 227 squat. Scientific and Technical Journals Sitk Rp, Branch in Krakow. 2012; 3(99): 349–363. (in Polish)
41. Kowalczyk D., Antolik Ł., Mikłaszewicz I. Railway rails disadvantages and ultrasonic tests. Nondestructive Testing and Diagnostics. 2019; 4: 9–13. (in Polish)
42. TORMAX – Comprehensive service of railway sidings: <http://tormax.com.pl/ceny-uslug-i-materialow/hurtownia-semafor/> attendance 2021.12.03.
43. Gómez-Guarneros M.A., Godínez-Salcedo J.G., Gallardo-Hernández E.A., Farfán-Cabrera L.I., Vite-Torres M. Corrosion rate and mechanisms of a rail head surface under artificial rainwater conditions. Materials Letters. 2021; 287: 129302.